Since January 2020 Elsevier has created a COVID-19 resource centre with free information in English and Mandarin on the novel coronavirus COVID-19. The COVID-19 resource centre is hosted on Elsevier Connect, the company's public news and information website.

Building and Environment 180 (2020) 107008

Contents lists available at ScienceDirect

Building and Environment

journal homepage: http://www.elsevier.com/locate/buildenv

Effects of personalized ventilation interventions on airborne infection risk and transmission between occupants

Chunwen Xu [a], Xiongxiong Wei [a], Li Liu [b,c,*], Li Su [c], Wenbing Liu [a], Yi Wang [c], Peter V. Nielsen [d]

[a] College of Pipeline and Civil Engineering, China University of Petroleum, Qingdao, 266580, China
[b] Department of Building Science, School of Architecture, Tsinghua University, Beijing, 100084, China
[c] State Key Laboratory of Green Building in Western China, Xian University of Architecture & Technology, Xi'an, 710055, China
[d] Department of Civil Engineering, Aalborg University, Aalborg, 9000, Denmark

ARTICLE INFO

Keywords:
Airborne disease control
Personalized ventilation
Exposure
Infection risk
Human microenvironment
Intervention

ABSTRACT

The role of personalized ventilation (PV) in protecting against airborne disease transmission between occupants was evaluated by considering two scenarios with different PV alignments. The possibility that PV may facilitate the transport of exhaled pathogens was explored by performing experiments with droplets and applying PV to a source or/and a target manikin. The risk of direct and indirect exposure to droplets in the inhalation zone of the target was estimated, with these exposure types defined according to their different origins. The infection risk of influenza A, a typical disease transmitted via air, was predicted based on a dose-response model. Results showed that the flow interactions between PV and the infectious exhaled flow would facilitate airborne transmission between occupants in two ways. First, application of PV to the source caused more than 90% of indirect exposure of the target. Second, entrainment of the PV jet directly from the infectious exhalation increased direct exposure of the target by more than 50%. Thus, these scenarios for different PV application modes indicated that continuous exposure to exhaled influenza A virus particles for 2 h would correspond with an infection probability ranging from 0.28 to 0.85. These results imply that PV may protect against infection only when it is maintained with a high ventilation efficiency at the inhalation zone, which can be realized by reduced entrainment of infectious flow and higher clean air volume. Improved PV design methods that could maximize the positive effects of PV on disease control in the human microenvironment are discussed.

1. Introduction

Exposure to pathogens from air has always been a major source of human morbidity and mortality worldwide. Influenza, for example, is one of the most common diseases that associate with human expiratory droplets and droplet nuclei, and the Centers for Disease Control and Prevention (CDC) reports that millions of illnesses and thousands of deaths are caused by seasonal influenza each year in the U.S [1]. Moreover, the 1918–1919 influenza pandemic caused 50 to 100 million deaths worldwide [1], and in 2009–2010 influenza A subtype H1N1 caused 17,000 deaths worldwide [2].

New pathogens emerge unceasingly. The current global pandemic of the 2019 novel coronavirus disease COVID-19 has caused over 2.9 million confirmed infections and over 200,000 deaths as of April 27, 2020 (24:00 GMT+8) [3]. The rapid spread of SARS-CoV-2, the virus that can lead to COVID-19, and the high level of morbidity associated with the COVID-19 epidemic has led to rapid and strict implementation of stringent control measures [4].

Of particular note is that the outbreaks of previous severe epidemics were found to be very closely related to transmission of infectious particles between persons in indoor environments [5], which highlights the importance of indoor environmental control. For example, Li et al. [6] reviewed several studies and found strong evidence of an association between ventilation and the transmission and spread of infectious diseases. Luongo et al. [7] also concluded that there was a causal link between factors related to building ventilation and the risk of disease transmission.

An increase in room ventilation rates is normally expected to decrease pathogen concentrations indoors, and such increases are used to reduce airborne infection risk. However, there is a lack of validated requirements for the use of ventilation to control the spread of airborne infectious diseases [6]. Jiang et al. [8] proposed that a safe ventilation

* Corresponding author. Department of Building Science, School of Architecture, Tsinghua University, Beijing, 100084, China.
E-mail address: liuli_archi@tsinghua.edu.cn (L. Liu).

https://doi.org/10.1016/j.buildenv.2020.107008
Received 13 February 2020; Received in revised form 30 April 2020; Accepted 23 May 2020
Available online 30 May 2020
0360-1323/

rate for eliminating airborne SARS-Co-V infection is to dilute the air emitted by a SARS patient 10,000-fold with clean air. The World Health Organization [9] suggested that a natural ventilation volume of 150 m^3/h per person is used in environments housing infectious patients. However, increasing the overall ventilation rate to such a high level would consume a large amount of energy, and total-volume ventilation of an entire room may not efficiently dilute infectious particles in the microenvironment between occupants [10,11].

Nevertheless, improving room ventilation efficiency is crucial, especially during epidemics or pandemics when there is a huge demand for ventilation volume. In this context, personalized ventilation (PV) that delivers clean air directly to a patient's breathing zone, thereby improving the ventilation efficiency for individual patients in the same room, may enable optimal infection control [10,12].

Bolashikov and Melikov [13] reviewed different ventilation strategies used for airborne disease control and proposed that PV may better protect occupants against airborne pathogens than total-volume room-air replacement. The American Society of Heating, Refrigerating and Air-Conditioning Engineers (ASHRAE) position document on airborne infectious diseases [14] also recommends PV and other ventilation strategies (such as dilution ventilation, local exhaust and source control ventilation) for use as effective measures to control and prevent disease transmission. This proposed strategy is in keeping with evidence that PV in conjunction with mixing ventilation (MV) can provide better protection against airborne infection than MV alone.

For example, Pantelic et al. [15] evaluated the performance of a desk-mounted PV air terminal device (ATD) and found that the PV ATD could reduce both the peak aerosol concentration and the exposure time of droplets that were released during coughing. PV coupled with underfloor ventilation was also reported to provide protection for seated occupants from exhaled infectious agents [16]. Habchi et al. [17] determined that a ceiling PV equipped with desk fans could reduce occupants' exposure to particles more than MV. Nielsen et al. [18] proposed that a bed-integrated PV with a textile pillow as a diffuser would exhibit a high degree of protection against cross infection. However, there is a limited amount of recent research on PV as an air distribution system for disease control. Furthermore, the use of different PV system designs, the varying locations of the infected sources, and the different methods used for infection risk-assessment have meant that no consistent design constraints for PV were developed in previous studies, which has restricted the practical application of PV.

Another important aspect is that in addition to the protective effect of PV, it may also facilitate the transport of exhaled particles, especially when people are located in close proximity wherein short-range airborne transmission can be significant [19,20]. This may mean that if an infected individual is situated in a PV zone but his/her fellow uninfected room occupants are not, the latter may suffer increased exposure to exhaled pathogens. For example, Li et al. [21] found that the provision of PV for only an infected source meant that the intake fraction of exhaled droplets was increased for an exposed person under MV conditions. This possibility of PV-facilitated transport of infectious pathogens was also addressed by Bolashikov and Melikov [13].

It can be expected that the protective effect of PV would be maximized when the occupant inhales totally clean air; this is dependent on the PV operating at high efficiency. PV is designed to directly interfere with a human microenvironment, which may exhibit complex flow interactions. This interacting flow may consist of a convective thermal boundary layer around the human body, exhaled flow from the infector, the general background ventilation and the PV flow supplied to the occupants [22,23]. The resulting complex flow interactions may affect the efficiency of PV and therefore also influence infective particle transmission within the microenvironment [12,22–28]. Consequently, low-efficiency PV systems may not effectively protect room occupants and may even increase occupants' risk of airborne infection.

The findings of several studies have indicated that PV protection technology can mitigate the spread of airborne transmissible diseases, but this research field is still developing. The objectives of this study were to experimentally investigate and estimate the effect of PV on the exposure and infection risk of a susceptible room occupant, and to further elucidate the causes of possible positive or adverse effects of PV on short-range airborne disease transmission between occupants. Based on the results, the potential and constraints of PV for infection risk-control are discussed.

Experiments were designed with a clean air supply of PV ranging from 3 L/s, 6 L/s to 9 L/s respectively to a source or/and a target manikin in close proximity (<1 m). Two scenarios were considered, with PV ATDs aiming at the inhalation zone of the occupant inclined at an upward or downward angle. Experiments were conducted in a full-scale room equipped with PV-integrated MV for mitigation of the spread of airborne transmissible disease. The effect of PV for an infector or/and a susceptible person was investigated with regards to exhaled droplets, which were released from a Collison nebulizer with an initial size distribution similar to human breathing and sampled by an aerodynamic particle sizer (APS). Two types of assessment methods based on droplet concentration measurements were used to assess the exposure to and the risk of infection with a certain disease, namely influenza A. The findings of this study will help guide the optimal design and application of PV for airborne infectious disease control.

2. Methods and design

2.1. Test room and facilities

Measurements were conducted in a particle-free environmental chamber of 5.0 × 3.5 × 2.5 m (L × W × H) equipped with MV, as shown in Fig. 1. To exclude the influence of particles contained in the room air

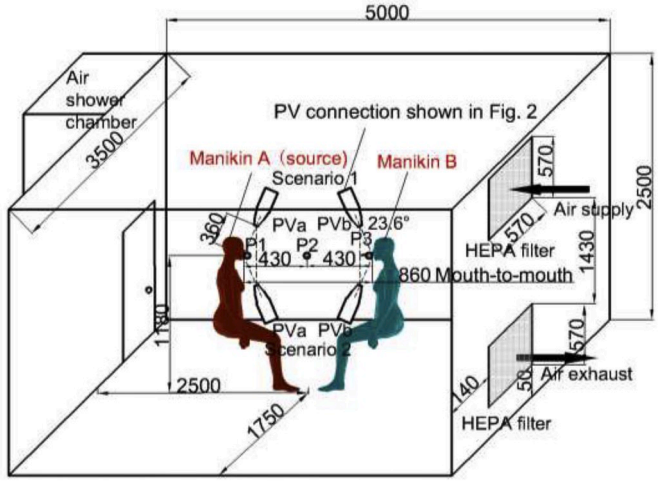

(a)

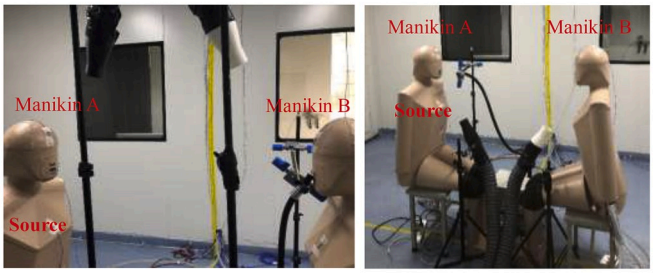

(b) (c)

Fig. 1. (a) Layout of the test chamber (units in mm); (b) scenario 1; (c) scenario 2. Manikin A acts as the infected source and Manikin B is the exposed occupant.

on measurements of tracer particles released from the infector, two high-efficiency particulate air filters (HEPA filters, 99.5%) were installed at the supply and exhaust openings, respectively, for realizing MV. The air-change rate (ACR) was set as 2 h^{-1}, equivalent to an air flow rate of 24.3 L/s. The cleanliness of the chamber was determined to be of ISO Class 7 standard [29]; to maintain this, both supplied air and return air were passed through the HEPA filter that was mounted behind the wall grille. The background concentration of the remaining particles was checked prior to experiments, and was thus excluded from calculations. Return air, which contained a small volume of fresh air, was treated at an air-handling unit. The supply air temperature was set at 16.5 ± 1.0 °C. The room air temperature and humidity were maintained by the conditioned supply air at 25.5 ± 1.0 °C and 36 ± 2% relative humidity (RH) during all experiments.

The respiratory activities of an infector, such as coughing, sneezing, talking and breathing, can generate droplets that contain infectious particles. To investigate this scenario, two breathing thermal manikins with a relatively complex body shape and breathing functions were used to realistically model human bodies and breathing processes. Manikin A served as the infected, breathing source (Fig. 1, left) and manikin B served as the exposed occupant (Fig. 1, right). More details about these manikins can be found in our previous studies [30,31]. The two manikins were placed face-to-face in sitting postures with a relative mouth-to-mouth distance of 0.86 m, which was used to represent a critical condition of a relatively short separation distance between two sedentary persons with the potential for direct contact. This critical face-to-face condition with a relative distance <1 m was considered to represent a realistic situation having a high possibility of short-range airborne transmission of airborne infectious particles, i.e., high cross-infection risk, such as on public-transport (e.g., buses or trains) or during doctor–patient interaction in a healthcare facility. These orientations were based on the fact that it has been shown that cross-infection is more likely between face-to-face oriented individuals than between face-to-back or back-to-back oriented individuals [32–34].

The manikins were set with a metabolic rate of 1.2 Met, representing persons engaged in sedentary activities. The breathing frequency and minute volume largely corresponded to the metabolic level of 1.2 Met, as shown in Table 1. Both manikins inhaled through the nose and exhaled through the mouth, but at opposite times: i.e., the target manikin inhaled at the same time as the source manikin exhaled, and conversely. This breathing pattern was considered of a higher infection risk compared with other patterns, as has been reported in Ref. [32,35].

Two PV nozzles were placed in front of the source (PVa) and the target manikin (PVb), respectively, pointing to their nose tips at a relative distance of 0.36 m and at an angle of 23.6° to the vertical direction. These dimensions were selected to ensure a relatively short distance between the two manikins. The relative distance of 0.36 m was selected to satisfy both the ergonomics considerations and a relatively high clean air volume. The PV jet was used to provide clean air directly to the manikins' inhalation zone and was thus the complement to MV.

Table 1
Parameters for the two manikins.

Parameters	Manikin A	Manikin B
Metabolic rate, Met	1.2	1.2
Heat output from the body [31], W/m^2	70	70
Breathing pattern	in nose, out mouth	in nose, out mouth
Breathing frequency, min^{-1}	15 (2 s exhalation–2 s inhalation within a breathing cycle)	15 (2 s inhalation–2 s exhalation within a breathing cycle)
Exhaled air flow rate, L/min	18.7 (3.9 from the nebulizer)	13.8
Inhaled air flow rate, L/min	13.8	14.8
Exhaled air temperature [30], °C	32.6 ± 1.0	30.5 ± 0.9 (Not heated by the electronic heater)

Fig. 2 depicts the setup of a PV. The flow rate of the nozzle jet was controlled and adjusted with a variable frequency fan and a manual damper. Three designed flow rates were applied: 3 L/s, 6 L/s and 9 L/s. An anemometer (TSI 9535A) was placed in a straight and relatively long circular cross-section air-duct to measure the exact flow rates of the PV, where this duct was 12 times longer than the diameter of the duct from the damper to the test point, as shown in Fig. 2. The velocity and concentration profiles of a similar convergent PV nozzle along a centerline were tested in Ref. [23]. The centerline velocity decay of the free nozzle jet with the tested flow rates was measured with a hotwire anemometer (Swema 03+) and the velocity profiles can be found in the Appendix (Fig. S1).

The PV system was mounted inside the test chamber, and supplied with recirculated room air. Specifically, recirculated isothermal room air was re-filtered by being passed through a custom-made HEPA filter mounted in the air duct of the PV and then supplied to the nozzle as clean particle-free air. The particle-free air chamber was well-sealed to avoid any inward leakage of particles from the outside, thus recirculated and finely filtered room air was used to supply the PV instead of external fresh air, to maintain the integrity of the test chamber and also to simplify the experimental system.

The initial turbulence intensity of the nozzle jet (at flow rates of 3 L/s, 6 L/s or 9 L/s) was measured with a hotwire anemometer (Swema 03+) and found to be less than 5%, and the length of the clean air core was 3–4 times the diameter of the nozzle (50.8 mm), both of which corresponded to our previous measurements [23]. It is preferable that a wider PV air terminal device (ATD) with a longer clean air core is used, as this can reach an occupant's breathing zone and therefore protect him/her from polluted room air. However, given that people vary widely in sizes, shapes and seating distances, and that they may adjust the position of the PV ATDs, it is unlikely that the use of PV can reliably offer optimal protection. Therefore, in this study a small nozzle was used to represent a situation wherein PV ATD supplies approximately 40% of clean air to the inhalation zone.

Fig. 3 presents the turbulent development of the PV flow with the same small nozzle aimed with a horizontal placement at a real person, and aimed with a downward or upward incline placement at the same manikin. It was found that with a nozzle-exit-to-target distance of approximately 0.4 m, this PV setup (Fig. 3) achieved a clean air delivery efficiency of approximately 40%, varying slightly with different placements of PV (horizontal, inclined upward or downward). Increasing the flow rate of PV from 3 L/s to 9 L/s increased the PV clean air-delivery efficiency by no more than 5% [23]. The horizontal placement of PV was not used in this study as it occupied too much shared space between the two face-to-face occupants. Instead, PV inclined upward or downward was used, as these placements achieved similar clean-air delivery efficiencies as the horizontal case.

To compare the effect of the positioning of PV, two scenarios were considered: nozzles placed above (scenario 1, Fig. 1 (b)) or below (scenario 2, Fig. 1 (c)) nose height. In both scenarios, PV may be performed with the PV ATD mounted on a movable arm-duct [12] attached to the top or the bottom of the room. The PV ATD can also be integrated with the ceiling or the desk to locate it close to the occupant. The concept of PV is to supply clean air directly to the breathing zone of a sedentary person, and to allow the exposed occupant and the infector some control of the flow rate and the flow direction. The infector may not be aware of his/her infection, and/or may only use PV when his/her health condition permits. Ten cases under two scenarios were tested (as shown in Table 2), which included the possibility of individual control of the PV flow rate.

2.2. Experimental procedures

The sensors and test equipment that were used and their specifications are listed in Table 3. To simulate multiphase flow consisting of

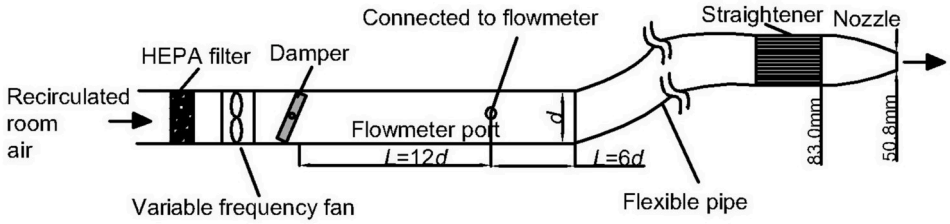

Fig. 2. Schematic of setup of the personalized ventilation (PV) device used for the two manikins (*d* is the inner diameter of the duct, which is 75 mm).

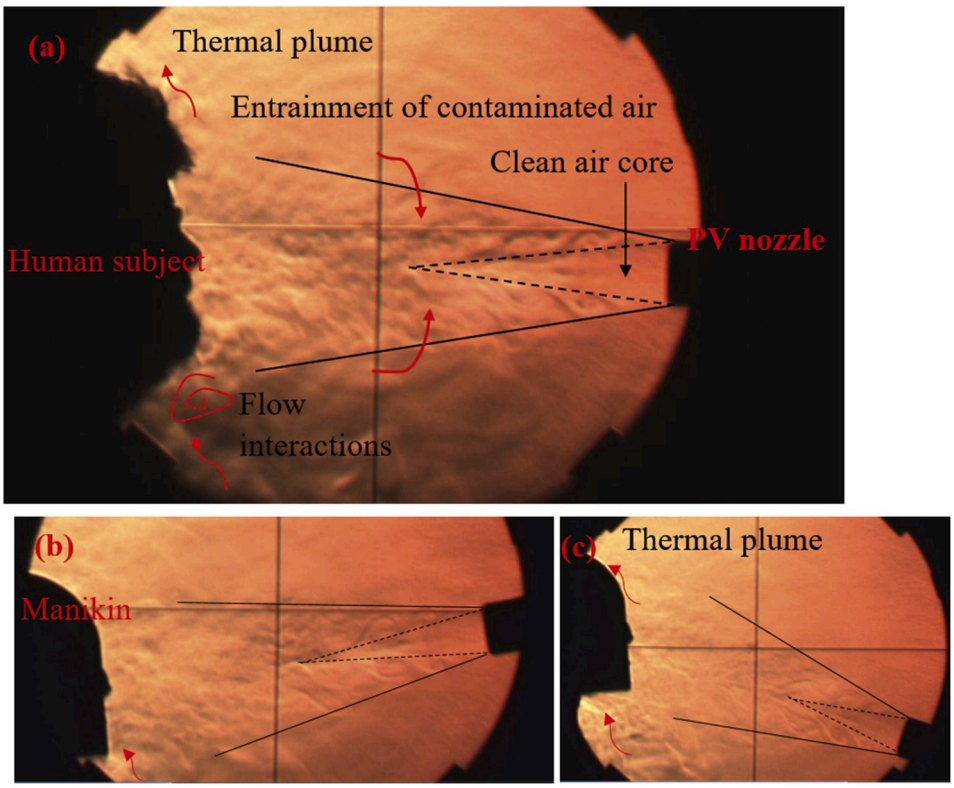

Fig. 3. Schlieren imaging visualization of the turbulent nozzle flow interacting with a human thermal plume [23]: (a) PV with a horizontal placement applied to a real person; (b) PV applied to a thermal manikin inclined downward and (c) inclined upward.

Table 2
Cases tested for the two scenarios.

Test series	Case label	PVa (L/s)	PVb (L/s)	MV[a](ACR[b])	$u_{P1,NM}$[c] (m/s)	$u_{P1,TM}$[d] (m/s)
Baseline case	MV	0	0	2	0	0
PV used for manikin A only	PVa3	3	0		1.14	0.56
	PVa6	6	0		2.28	1.40
	PVa9	9	0		3.48	2.19
PV used for manikin B only	PVb3	0	3		0	0
	PVb6	0	6		0	0
	PVb9	0	9		0	0
PV used for both manikin A and B	PVab3	3	3		1.14	0.56
	PVab6	6	6		2.28	1.40
	PVab9	9	9		3.48	2.19

[a] MV: mixing ventilation.
[b] ACR: air change rate.
[c] $u_{P1,NM}$ is the PV centerline velocity of a free nozzle jet at P1 (the distance between the nozzle and P1 is 0.36 m) with Manikin A absent (NM), which was measured using a hot wire anemometer (Swema 03+).
[d] $u_{P1,TM}$ is the PV centerline velocity at P1 with Manikin A present (TM), which was extrapolated from Fig. 6 in Ref. [23].

expiratory droplets suspended in expelled air from the infected person, a Collison nebulizer (3-jet, BGI, Inc., Waltham, MA) was used to generate polydisperse droplets. With appropriate settings of the flow rate of supplied air and solution of the liquid, this nebulizer can produce similar droplet size distribution profiles to human breathing. The pressure of clean and compressed air supplied to the nebulizer was set as 10 psig (0.069 MPa), corresponding to an aerosol generation flow rate of 3.9 L/min. Sodium chloride (NaCl) served as the core of droplet nuclei in human breathing [36] and 50% distilled water mixed with 50% isopropyl alcohol by volume was used as the solvent to simulate the evaporable components in human saliva. The density of the solution was 33.8 μg/mL. The droplet size-distribution profiles between human breathing and the nebulized aerosols in this study are compared in Table 4.

Fig. 4 depicts one example of the sampled droplets from the manikin's mouth P1. The geometric mean diameter and the modal diameter of the generated droplets were 0.7 μm and 0.6 μm, respectively, with a geometric standard deviation varying from 1.22 to 1.35. This confirmed that this solution could be used to generate a similar droplet size-distribution profile to human breathing [38].

The droplets released from the nebulizer were injected into the exhaled air of the source manikin (manikin A) and were then expelled at

Table 3
Key experimental equipment and specifications.

Equipment	Manufacturer and model	Sensitivity and/or technical data	Error
Aerodynamic particle sizer	TSI Model 3321	Aerodynamic particle size range: 0.5–20 μm; Resolution: 0.02 μm at 1.0 μm diameter and 0.03 μm at 10 μm diameter; Display resolution: 32 channels per decade of particle size (logarithmic); Sampling time: 1 s.	±10% of reading plus variation from counting statistics.
Collison nebulizer	BGI, Inc. 3-jet	Pressure (this study): 10 psi; Volume of air: 3.9 L/min; Liquid loss (droplet + vapor): 9.15×10^{-3} mL/min.	GSD[a]: 1.22-1.35
Omnidirectional anemometer	Swema 03+	Velocity range: 0.05–3 m/s at 15–30 °C (can be expanded to 10 m/s); Response time: <0.2 s; Maximum sampling frequency: 100 Hz	±0.03 m/s at 0.05–1.0 m/s; ±3% read value at 1.0–3.0 m/s
Hotwire anemometer	TSI 9535A	Velocity range: 0–30 m/s; Resolution: 0.01 m/s; Response time: 1 s.	The maximum of ±3% read value or 0.015 m/s.
Thermocouples	Type K	Temperature range: 0–50 °C	±0.1 °C

[a] GSD: Geometric standard deviation.

a designed frequency and temperature (Table 1) from the manikin's mouth. It was expected that droplet deposition would occur in the manikin's respiratory airway, which would result in particle loss before the exhalation flow arrived at the manikin's mouth. However, as only droplets released from an occupant's mouth would contribute to infectious particle transmission indoors, the deposition or the subsequent resuspension process occurring in the manikin's respiratory airway was ignored. Accordingly, the particle concentration measured at the mouth opening was used as the initial concentration for further analysis. However, the nebulizer-generated initial droplet concentration was found to be higher than that from humans, and thus should be normalized by the average initial concentration from human subjects' mouth breathing for further infection-risk assessment.

The time required for droplets to evaporate from their initial condition to nuclei was expected to be very short, but depends on many factors [39–42]. Based on the calculation suggested by Nicas et al. [42], it was found that 0.1 s would be required for droplets with an initial size of 12 μm to evaporate to nuclei. Therefore, we expected that instantaneous evaporation occurred before the aerosolized droplets reached the manikin's mouth via the tube inside the manikin's body. Fig. 4 shows one of the examples of the sampled particle size distributions at the source manikin's mouth. It can be seen that the geometric mean aerodynamic particle size is approximately 0.7 μm, with more than 80% of droplets smaller than 1 μm, which means that for short-range transmission, the deposition rate of aerosols from mouth breathing is negligible. Duan et al. [43] determined that the deposition rate of 1 μm-diameter droplets on the facial mucosa of the droplet-generating person was only 1.02%, implying that airborne transmission could be a dominant mode of short-range transmission [20].

Measurements of the numbers of droplets in the microenvironment between the two manikins were conducted with an APS (TSI model 3321), which measures the aerodynamic diameter of particles in the diameter range of 0.5–20 μm and detects particles as small as 0.3 μm. The sampling time interval was set as 1 s. An APS has been used in several studies [38,44] for detecting the initial droplet size-distribution in human respiration. An isokinetic probe was positioned in the inhalation zone of the target manikin, 10 mm below the nose (P3 in Fig. 1). Concentration measurements were also taken at the source manikin's mouth (P1 Fig. 1) and at the center point between the two manikins (P2 Fig. 1). An additional omnidirectional hotwire anemometer (Swema 03+) was used in the center vertical plane to determine the position of P2 at maximum velocity, representing the centerline position of the exhaled flow [30,31,34] from the infected person.

2.3. Criteria for assessment

2.3.1. Exposure risk assessment

The source expelled droplets with a time-averaged level of S, which can be derived from Eq. (1), where C_s is the measured concentration at P1 at the mouth opening of the source manikin, as follows:

$$S = \frac{\int_0^\tau C_s d\tau}{\tau} \quad (1)$$

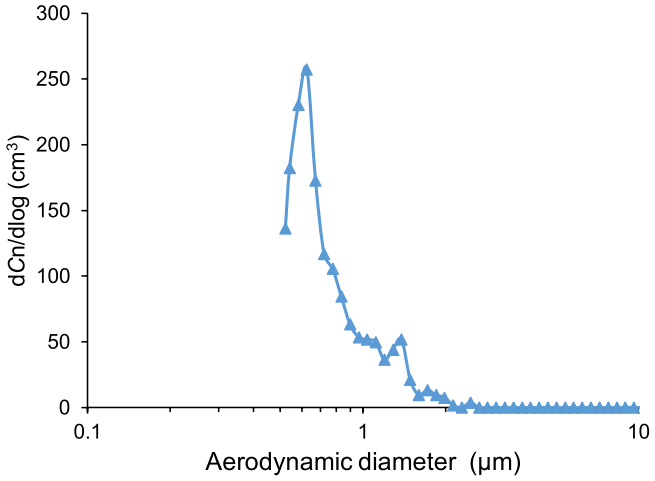

Fig. 4. One example of the particle size distribution at the source manikin's mouth.

Table 4
Experimental expiratory-droplet size data.

Study	Expiration type	Measurement technique	D_{min} [μm]	D_{max} [μm]	Geometric mean [μm]	Geometric standard deviation [μm]
Papineni and Rosenthal [36]	Mouth breathing	OPC[a]	<0.6	2.5	0.7	1.4
Papineni and Rosenthal [36]	Nose breathing	OPC[a]	<0.6	2.5	0.8	1.5
Papineni and Rosenthal [36]	Mouth breathing	ATEM[b]	<0.6	2.5	1.2	1.6
Edwards et al., 2004 [37]	Breathing	OPC[b]	/	/	Predominant size is 150–199 nm	/
Morawska et al. [38]	Mouth breathing	APS[c]	<0.3	5.5 ± 1	Modal diameter <0.8	/
This study (see Fig. 4)	Mouth breathing	APS[c]	<0.5	2.5–5	0.7	1.22–1.35

[a] OPC: optical particle counter.
[b] ATEM: analytical transmission electron microscope.
[c] APS: aerodynamic particle sizer.

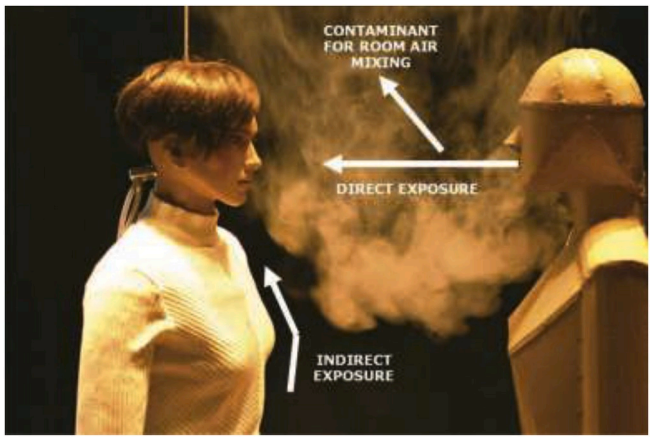

Fig. 5. Contaminant flow between the source (right) and target (left) manikins indicated by smoke [47].

The room was supplied with MV at a constant air-flow rate q_0. The concentration in the exhaust of the room C_e is thus expressed in Eq. (2) [45] as follows:

$$C_e = \frac{S}{q_0} \tag{2}$$

The concentration of droplet nuclei in the breathing zone of the target manikin C_{bz} is normalized to yield an exposure risk index [46], defined in Eq. (3) as follows:

$$\varepsilon_{bz} = \frac{C_{bz}}{C_e} = C_{bz}\frac{q_0}{S} \tag{3}$$

When $\varepsilon_{bz} = 1$., PV delivers no clean air to the breathing zone, representing pfectly mixed conditions; when $\varepsilon_{bz} > 1$, the proportion of exhaled droplets in the target's breathing zone is greater than in the ambient environment; and when $\varepsilon_{bz} < 1$, PV can protect the exposed occupant from the exhaled droplets to some extent, which is the preferable condition. It may be possible to reduce the inhaled concentration of droplet nuclei by using a high flow rate of ventilation q_0 to dilute the overall infectious particle concentration in the entire system. However, the localized concentration in the microenvironment between the occupants may not be efficiently and effectively diluted by the general ventilation [10,11].

As shown in Fig. 5, the localized concentration C_{bz} in the inhalation zone of the target is not only derived from indirect exposure $C_{indirect}$ but also from direct exposure C_{direct} [47]. Indirect exposure is generated by transport and dilution of the exhaled contaminant from the source by the general ventilation, whereby the exhaled contaminant flows to the room and attains a concentration distribution around the target person. Direct exposure occurs by exhalation from the source flowing directly into the target's breathing zone. Thus, two additional exposure-risk indexes can be defined as Eqs (4)–(6):

$$\varepsilon_{indirect} = \frac{C_{indirect}}{C_e}\ . \tag{4}$$

$$\varepsilon_{direct} = \frac{C_{direct}}{C_e} = \frac{C_{bz} - C_{indirect}}{C_e} \tag{5}$$

$$\varepsilon_{bz} = \varepsilon_{indirect} + \varepsilon_{direct} \tag{6}$$

All of the measurements were conducted after a few hours of MV, when the pticle concentration in the exhaust had reached a relatively steady state. APS-based measurement of C_{bz} lasting for 10 min generated 600 samples of instantaneous particle concentration. $C_{indrect}$ w obtained by measurement at the same sampling point as C_{bz}, immediately after shutting down the exhalation of the source. The sampled particle concentration in the breathing zone was thus only from the air distribution around the target.

A 10-min sampling period was also used for the measurement of $C_{indrect}$. There might be a decrease of $C_{indrect}$ over time without the release of particles from the source, but it can be inferred that the overall concentration of tracer particles in the room would decay by less than 8% in an exponential function over time under an ACR of 2 h^{-1}. Given that the microenvironment between the occupants might not be diluted efficiently by the general ventilation, the decay of $C_{indrect}$ during the short sampling period was not considered.

2.3.2. Infection risk assessment

Another index to evaluate infection risk under PV was used. The advantage of using tracer particles as media to simulate pathogen transport is that the infection risk of certain diseases such as influenza A can be evaluated by using the exposed droplet concentration in the breathing zone of the susceptible person. Based on the dose-response model for an unsteady imperfectly mixed environment [48], the probability of infection can be estimated using Eq. (7) [49]:

$$P_1(t_0) = 1 - exp\left(-\sum_{j=1}^{m} r_j \beta_j c p q t_0 \int_0^{t_0} v(t)_j f\left(t\right) dt\right) \tag{7}$$

where $P_1(t_0)$ is the probability of infection of the susceptible person, m is the total number of size bins, $v(t)_j$ is the volume density of droplets of the jth size bin, and β_j is the deposition fraction of the infectious particles of the jth size bin. The exposure level is divided into different size bins based on the consideration that the infectivity varies with particle size and deposition site in the respiratory tract [50]. Furthermore, r is a fitting parameter to make $P_1(t_0)$ equal to 0.5 when the infectious dose is ID_{50}, c is the pathogen concentration in the respiratory fluid [49], q is the breathing frequency of the infector, p is the pulmonary ventilation rate of the susceptible person, t_0 is the exposure time interval, $f(t)$ is the viability time-function of the pathogen, and $v(t)_j$ is the volume density of expiratory droplets in the exhalation of the infector.

The expiratory droplets evaporate and shrink to nuclei within a short time [39–42]. The concentration of droplet nuclei can be measured at

Table 5
Literature data used for calculation of the infection risk of influenza A.

Parameter	Influenza A	Remarks
c	1×10^5 $TCID_{50}$[a]/mL	Geometric mean from seven patients (Murphy et al., 1973 [51])
Respiratory deposition and infectious dose	$ID_{50} = 1.8TCID_{50}$ $r = 0.385$[b]	Infectious dose for aerosol ≤3 μm, mean value of the range: 0.6–3.0; $\beta = 0.6$ (Alford et al., 1966 [53])
	$ID_{50} = 223.5TCID_{50}$ $r = 0.0031$	Upper respiratory tract infectious dose, for larger aerosol mean value of the range: 127–320 reported by Douglas (1975) [54]; β, total respiratory fraction reported by Hinds (1999) [48]
Viability of influenza virus	<20 °C and 60% RH approximately 20% remained viable at $t = 0$, $f(t) = 0.0351e^{-0.261t}$	Extrapolated from Fig. 6 in Hemms et al.(1960) [55]
$v(t)_j$	Assume final nucleus size represents 6% of the initial volume (Nicas et al., 2005 [42])	Calculation given by Sze To et al. (2008) [49]

[a] $TCID_{50}$ refers to the mean tissue-culture infectious dose, a unit to describe the quantity of virus.
[b] $r = 0.385$ is used for calculation as the infectious dose is for aerosols of ≤3 μm (Fig. 4).

the inhalation zone of the target manikin and the droplet nuclei sizes are adopted for β_j and r_j. The nucleus sizes of aerosols should be converted to their initial droplet sizes to calculate $v(t)_j$, as c refers to the pathogen concentration in the respiratory fluid before evaporation.

The volume density of expiratory droplets in the exhalation of the infector, $v(t)$, can be derived from the measured concentration in the breathing zone of the susceptible person, C_{bz} [49]. As the initial concentration of droplets released from the source manikin was higher than those from real persons, the initial aerosol concentration, C_0, measured at the mouth opening of the source manikin (P1 Fig. 1) was normalized to an average initial concentration of 0.092/cm^3, which was in line with the data obtained by APS analysis of human subjects breathing [38]. The C_{bz} was then normalized with respect to the ratio between C_0 and 0.092/cm^3, and was used for further infection-risk assessment.

The infection risk of a common airborne-transmitted virus, which causes influenza A, was evaluated under the effect of PV. Influenza A viruses are nanometer-scale biological particles that can infect both the upper and lower respiratory tract. The aerosol transmission of influenza virus has been estimated as one of its most dominant transmission pathways in some studies [51,52]. Epidemiological data from previous infection-risk assessments for influenza A are given in Table 5.

3. Results

The results were obtained from the measurement point P3 (indicated in Fig. 1), which was in the inhalation zone of the manikin and affected by different types of airflows. The flow field in the occupant's inhalation zone consisted of complex interactions between the following: the general ventilation of MV, the PV-generated flow, the buoyancy-driven thermal boundary layer around the occupant, the inhalation/exhalation flow from the occupant, and the exhaled flow containing droplets from the infected person. The complex airflow interactions between the PV and the thermal boundary layer were studied previously by the authors, using tracer gas (N_2O) measurement, Laser Doppler Anemometry (LDA) and Schlieren imaging techniques [56]. In this study, emphasis was placed on the importance of the combined effect of PV, exhaled flow from the infector and the inhalation of the susceptible person on airborne transport of infectious particles.

3.1. Exposure risk assessment for scenario 1

Figs. 6 and 7 show the exposure risk ε_{bz} and indirect exposure risk $\varepsilon_{indirect}$ for the scenario 1 test series in Table 1, respectively. Fig. 7 depicts the indirect exposure without measuring cases of PVab. It can be seen that C_{bz} of the baseline case of MV was slightly higher than C_e with ε_{bz} slightly higher than 1, indicating slightly higher droplet concentrations were present in the microenvironment between the occupants than the ambient air. This corresponded to the results in Ref. [34] under MV with a relative distance >0.8 m. The initial exhaled velocity produced by the

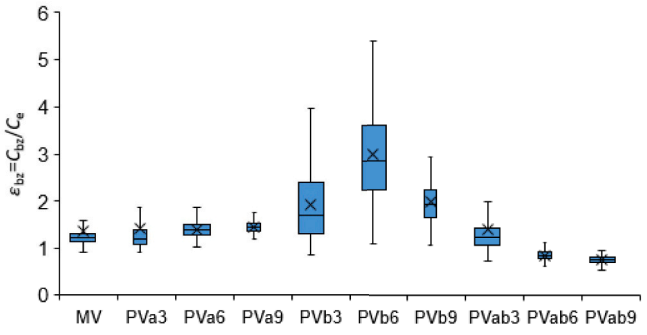

Fig. 6. Box plot of exposure risk ε_{bz} in the breathing zone of the target manikin for scenario 1.

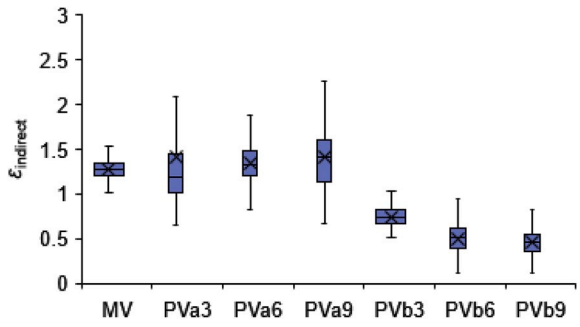

Fig. 7. Box plot of indirect exposure $\varepsilon_{indirect}$ in the breathing zone of the target manikin for scenario 1.

artificial lung from the source manikin's mouth was approximately 2.44 m/s and the centerline velocity decayed to 0.32 m/s at the vertical P2 plane (0.43 m apart from the mouth). The centerline of the exhaled flow was found to bend upward, 5 cm higher than the mouth height. It can be inferred that the direct influence of the source manikin's exhalation flow was negligible in the inhalation zone of the target manikin, as under these conditions both the exhaled velocity and concentration would decay to approximately background values with a separation distance of 0.86 m [30,31]. This can also be seen from Figs. 7–9(a), where the indirect exposure $\varepsilon_{indirect}$ was comparable to ε_{bz} with MV, accounting for an average of 94.2% total exposure.

When the source manikin was subject to PV, indirect exposure was still dominant, with an average proportion of 96.2–98.1% of the total exposure (Figs. 8 and 9(b)). Fig. 6 shows that the ε_{bz} with PVa was slightly higher than that with MV and no significant correlation with the flow rates of PVa was found. Due to the downward supply of PVa to the breathing zone of the source manikin, the exhaled flow interacted with the PV jet immediately after it left the mouth opening (Fig. 9(b)), and thus the mixing effect of the exhaled droplets with the forced convection of PV was enhanced. The development of the exhaled flow was inhibited by PV, especially at higher PV flow rates of 6 L/s and 9 L/s in which the centerline disappeared and the centerline velocity was unmeasurable. However, the exhaled flow was able to penetrate the 3 L/s PV flow, whose centerline velocity was measured to be 0.22 m/s and was 3.5 cm higher than the mouth height at the P2 plane. This was because the penetration velocity was significantly higher than the received PV velocity at the mouth. The maximum exhaled velocity from the mouth was approximately 2.44 m/s and the PV centerline velocity decayed to merely 0.56 m/s at a distance of 0.36 m from the nozzle [23]. As the PV was oriented toward the nose, the velocity of the PV at the mouth away from the centerline would be even less than 0.56 m/s.

Fig. 6 also shows that unexpected transmission of droplets could

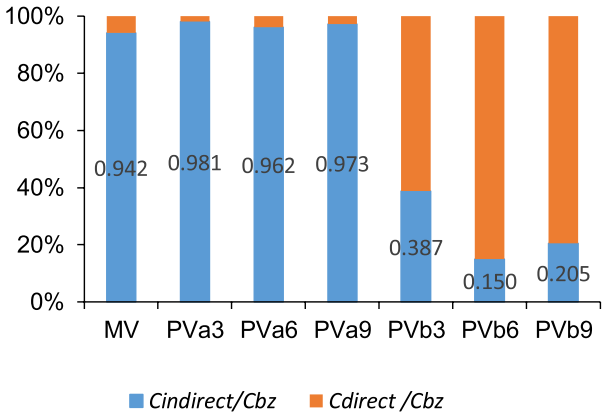

Fig. 8. Time-averaged proportion of direct and indirect exposure in the breathing zone of the target manikin for scenario 1.

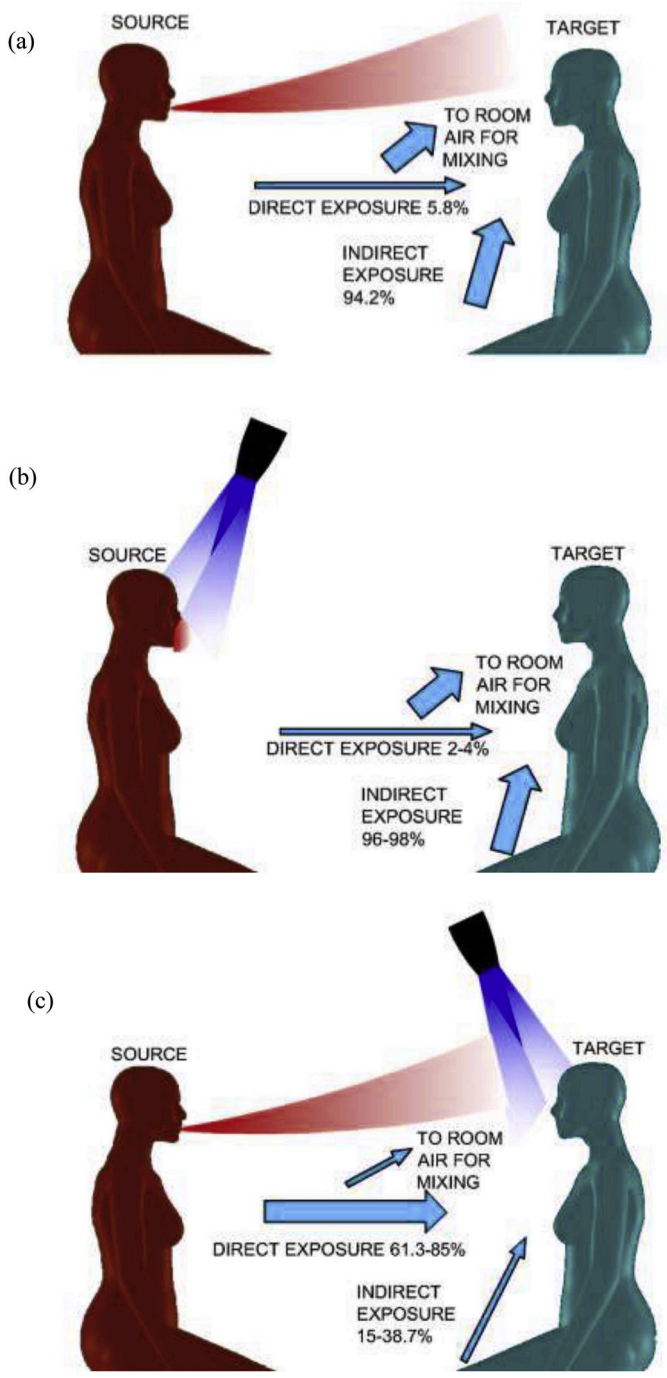

Fig. 9. Airborne transmission between the two occupants with (a) MV, (b) PVa – scenario 1 and (c) PVb – scenario 1. The volumes of the exhaled flow and the PV jet are depicted according to the flow visualization and measurements in Fig. 3 and [56].

occur when PVb was used. The ε_{bz} and its fluctuations with PVb were significantly higher than those with MV or PVa. The higher fluctuations of ε_{bz} may be caused by the dynamic interactions of PV with the periodic exhaled airflow, especially for PVb of 3 L/s and 6 L/s. The ε_{bz} was elevated as the droplet-laden exhaled flow grew with propagation distance, reached the accessible area of PV flow and was then entrained by PV. The exhaled droplets were taken directly to the inhalation of the exposed manikin by the PV air.

However, when the source manikin was inhaling, the droplets would not be directly loaded by the PV air and the ε_{bz} would be less. The ε_{bz} reached a maximum value of 5.4 (Fig. 6, PVb 7 L/s), but the averaged $\varepsilon_{indirect}$ for all PVb cases were less than 1 and even lower than those in the MV case (Fig. 7). This meant that the direct exposure largely contributed to the elevated exposure risk via PVb. Fig. 8 shows the direct exposure accounted for 61.3–85% of the total exposure when PVb was used. This can be explained by the PVb-accelerated transport of droplet nuclei to the occupant's breathing zone. With the development of the nozzle jet, droplet-laden ambient air was entrained within vortex rings in the turbulent shear layer. The concentrations of these droplets could increase when the entrained air was directly drawn from the droplet-laden exhalation flow. Fig. 9(c) shows that the end edge of the exhaled flow may collide with the turbulent nozzle jet and lead to high concentrations of droplets in the PV air. However, the highest concentrations of droplets occurred with PVb 6 L/s rather than 9 L/s. This was probably due to increased clean volume of PV flow at the flow rate of 9 L/s.

The air quality of the nozzle jet deteriorated with the development of the flow. When both of the occupants were subject to PV, the deterioration of the PVb flow was significant at a low air flow rate of 3 L/s. As the exhaled flow could penetrate a PVa flow of 3 L/s, the PVb contained the same concentration of droplets as the room air. An approximately 40% proportion of clean air could be directly supplied to the inhalation zone of the susceptible person at higher flow rates of 6 L/s and 9 L/s.

3.2. Exposure risk assessment for scenario 2

The measurement results for scenario 2 are presented in Figs. 10–13. When the source manikin used PVa, it was observed that the exhalation flow was able to penetrate the supplied PV flow of 3 L/s. The centerline velocity of exhaled flow at P2 plane was found to be 0.24 m/s (9.8% of the initial velocity) and 7 cm above the mouth height, which also exceeded the nose height of the target. The centerline of the exhaled flow was somewhat elevated by the upward air stream of PVa.

When PVa was operated with 6 L/s or 9 L/s, the centerline of exhaled flow disappeared at the P2 plane, and the mixing of exhaled droplets with PV air occurred in the breathing zone of the source manikin. Therefore, the contamination of the inhaled airflow of the target manikin largely depended on indirect exposure. The average ε_{bz} of PVa was slightly greater than 1, approximately the same as that under MV, indicating that complete mixing occurred in the inhalation zone of the target. The proportion of indirect exposure to total exposed droplets was greater than 94%, slightly greater than that for 3 L/s.

As both the exhaled flow and the PVb air developed an upward direction as shown in Fig. 13(b), the collision between the PV jet and the end part of the exhaled flow or the remaining suspended cloud of particles after exhalation was not as marked as that which occurred in scenario 1. A smaller proportion of exposed droplet nuclei was derived from direct exposure (56.7–72.7%) than that in scenario 1 (61.3–85%), but still more than 50% of the inhaled droplet nuclei were directly delivered from the exhalation of the source. Thus, the use of PVb led to an increased exposure level and turbulence intensity in the inhalation

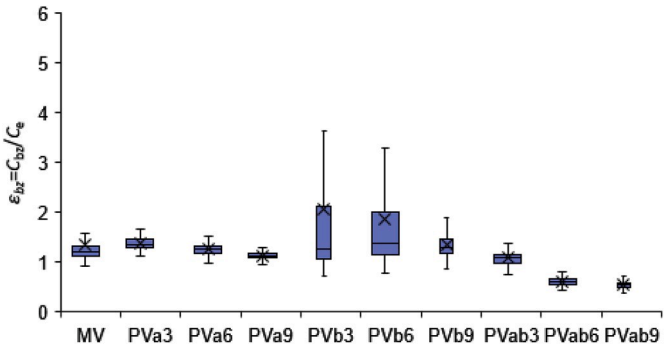

Fig. 10. Box plot of exposure risk ε_{bz} at the breathing zone of the target manikin for scenario 2.

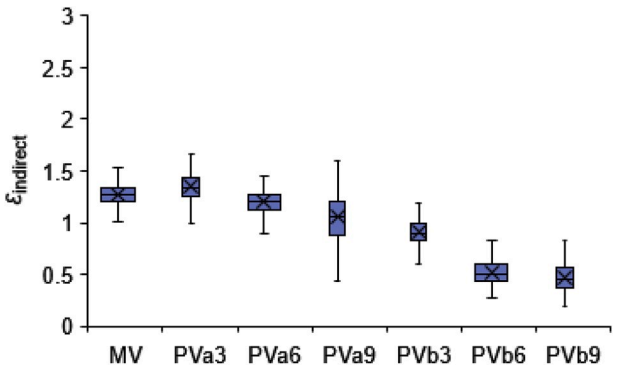

Fig. 11. Box plot of indirect exposure $\varepsilon_{indirect}$ at the breathing zone of the target manikin for scenario 2.

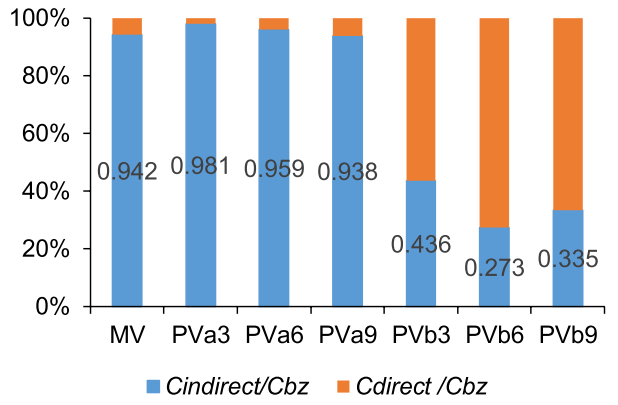

Fig. 12. Time-averaged proportion of direct and indirect exposure in the breathing zone of the target manikin for scenario 2.

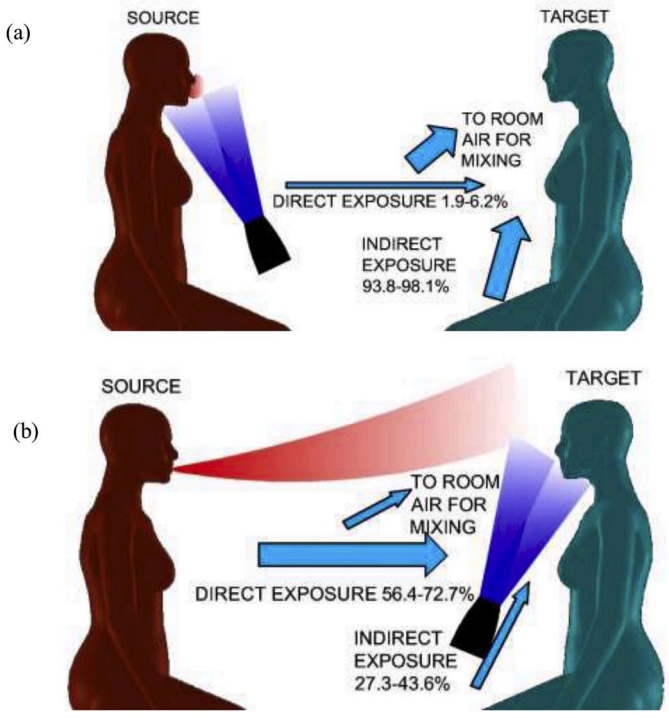

Fig. 13. Airborne transmission between the two occupants with (a) PVa – scenario 2 and (b) PVb – scenario 2. The volumes of the exhaled flow and the PV jet are depicted according to the flow visualization and measurements in Fig. 3 and [26].

zone of the target manikin. This implies that improper placement of PV for the susceptible person may have an adverse effect on infection control, especially when the PV flow may closely interact with the exhalation from the infector. That is, direct turbulent entrainment of exhaled droplets to the PV flow would cause rapid deterioration of the clean PV air, and thus a greater concentration of droplets would be delivered to the breathing zone of the occupant. Although increasing the flow rate resulted in the clean PV air compensating for this deterioration, this strategy led only to a limited improvement in air quality in the inhalation zone of the target, as shown in Fig. 10 of PVb.

It should be noted that the exhalation of human breathing may not penetrate as far as the exhalation of such manikins, and thus the human exposure risk may be somewhat overestimated by these data [30]. Specifically, it has been found that the high initial turbulence intensity at the mouth opening, caused by humans' complex respiratory tract [30, 57], results in the maximum propagation distance of exhaled flow being less than that from a manikin [30]. In addition, most measurements of mouth breathing in human subjects found a downward flow trend with an average angle of 14° [56]. Appendix Fig. S2 presents an example of a human subject's mouth breathing. The upward PVb jet used in scenario 2 may thus also entrain infectious pathogens from human exhalation flow bending downward. Therefore, the placement of PV for the susceptible person within the infectious particle-exposure zone between the occupants should be avoided, as PV directed to this area may actually lead to a heightened infection risk. Apparently, the separation distance of 0.86 m was not sufficient for the use of PV for the two face-to-face occupants, and thus the minimum distance required for the placement of PV to control infectious particle transmission should be further investigated.

The application of PV to the infector would accelerate the mixing of infectious particles with room air and indirect transmission would be the dominant mode of particle transport. In Fig. 10 a comparison of PVab with PVb indicates that PVb effectively protected the susceptible person only when it was placed away from the high-concentration droplet flow and was realized with a relatively large amount of clean air.

3.3. Infection risk of influenza A

Infection-risk assessment is a useful tool for studying disease transmission and evaluating the effectiveness of infection-control measures [33]. Fig. 14 shows the predicted infection risk of influenza A over an exposed time interval ranging from 10 min to 2 h. The results were obtained based on the epidemiological data in Table 5. The exposure risk of an individual indicates the relative scale between the exposure concentration of an infectious agent and that contained in ambient air, as expressed in Eq. (3). The infection probability modeled by the dose-infection relationship in Eq. (7) consists of the estimation of the infection-dose intake, which requires knowing the absolute level of exposure to the infectious agent. The mean intake-dose value should be used rather than the value of a single trial for the risk calculation, because the variability of intake dose has been incorporated in Eq. (7) using the Poisson probability concept [58]. The infection probability $P(t)$ can be inferred to increase with the mean relative exposure level ε_{bz}, but slight differences may also exist between the trends of these parameters under different ventilation modes. As shown in Fig. 14, cases with PVb of 6 L/s had the highest influenza A infection risk in both scenarios. This was due to that fact that the modeling of infection risk not only considers the absolute aerosol concentration C_{bz} but also takes into account the size distributions of both the inhaled droplet nuclei and the initial expiratory droplets.

From the results in Fig. 14, it can be seen that PV has the potential to either increase or decrease the infection risk of influenza A in both scenarios. The results also show that increasing the PV flow rate does not always effectively control the infection risk. That is, the increase of infection risk with PV compared with that with MV was caused by PV causing increased indirect and/or direct exposure level to the

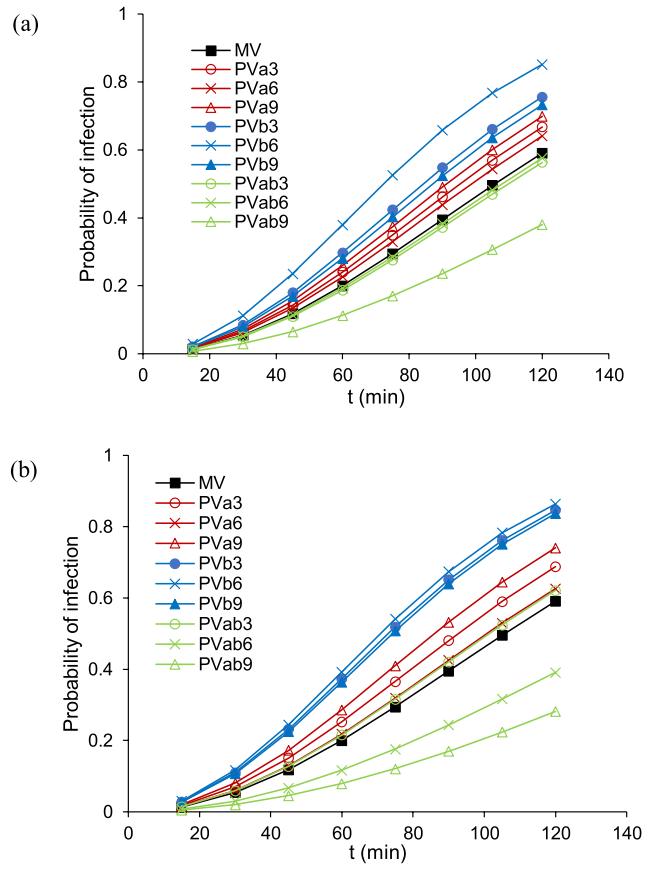

Fig. 14. Infection risk-assessment of influenza A over time in (a) scenario 1 and (b) scenario 2.

susceptible person. The application of PV to the infectious source may therefore in some circumstances accelerate the mixing of infectious particles with room air and may increase the indirect exposure to the person who shares the same room space, but in this situation the increase in infection probability was estimated to be no more than 0.15 within the calculated exposure interval of 2 h.

When the PV flow developed in the infection-prone zone between the occupants, rapid deterioration of the PV air would probably introduce even more infectious particles directly into the inhalation, which obviously should be avoided in practical design. For a short exposure time interval, e.g., 30 min, the infection probability was less than 0.1 and did not vary much among different alignments of PV. With continuous contact with the infectious particles for over 2 h, the infection probability could exceed 0.85, which equates to a high possibility of infection for the susceptible person. If the intake dose was well controlled and maintained at a low level, the infection risk over 2 h would be minimized to approximately 0.28 by use of PV, as shown in Fig. 14 (b). This implies that PV may offer protection against airborne transmission only if clean and fresh air is successfully supplied to the inhalation zone of the occupant. This was achieved with PVab of 9 L/s for both scenarios and with PVab of 6 L/s for scenario 2; moreover, PVa values of 6 L/s and 9 L/s suppressed the development of the infectious exhaled flow.

Conversely, PV may aid in the transmission of infectious particles when it closely interacts with the exhaled flow from the infectious source. For example, when PVa was 3 L/s, the exhaled flow could penetrate the invading PV flow, and thus these PV conditions did not protect the exposed occupant.

To summarize, the performance of PV used for infection-risk control depends largely on the extent to which PV entrains infectious droplets from its working environment. That is, PV used for the infector facilitated the transport of airborne particles but the increased indirect infection risk was found to be limited in ventilated space. Nevertheless, direct entrainment of an infectious exhaled flow by PV should be strictly avoided.

With respect to the design of PV required to protect against airborne transmission, the following aspects should be considered: (1) PV should be carefully oriented away from an adjacent occupant's breathing zone; (2) high efficiency PV with reduced entrainment of ambient particle-laden air is preferable; and (3) a higher volume of clean air from PV can be also be protective, but only when it does not interact with the adjacent occupant's exhaled flow.

4. Discussion

4.1. Improved PV designs for disease control

As PV is a ventilation mode that directly interferes with a human microenvironment, the flow interactions within this microenvironment should be carefully considered to identify the best design for optimal infection control. Advanced PV designs should be developed to satisfy requirements for effective interventions in airborne transmission pathways at any point within the microenvironment, from where particles leave the infectious source to where these enter the breathing zone of another.

In this study it was found that the effectiveness of PV in protecting against infectious particle transmission largely depends on the extent to which PV entrains ambient infectious particles. If low entrainment of ambient air by PV can be realized, PV can deliver clean air with high efficiency directly to the breathing zone of the exposed occupant. PV ATDs with wider diameter that can achieve a longer clean air core are recommended for this purpose. When the jet's clean-air core is long enough to reach the occupant's breathing zone (BZ), the occupant can be effectively protected. Khalifa et al. [59,60] designed a novel co-flow nozzle to lengthen the inner clean-air core of the inner primary nozzle for improving the achieved air quality at the BZ with use of a small fraction of clean air. This can also be easily realized by using PV ATDs placed in close proximity to the BZ. Some PV ATDs are therefore designed based on this close-to-BZ concept. For example, Bolashikov et al. [61] and Melikov et al. [62] each reported a high efficiency PV nozzle placed at each side of the headrest, which would supply up to 99% clean air to the BZ. Niu et al. [63] proposed a chair-based PV ATD design with the PV nozzle placed just beneath the mouth at the microphone position, which could achieve up to 80% fresh air in the inhaled air with a supply flow rate of less than 3.0 L/s.

A desk-mounted round movable arm proposed by Bolashikov et al. [64] can also realize a high clean-air delivery efficiency due to the short distance between the PV ATD and the BZ. Nielsen et al. [18] reported an entrainment-minimized PV ATD to improve inhaled air quality; this does not use the jet entrainment concept but locates the source of clean air in the boundary layer close to the BZ. This idea was based on the body's close contact with textile surfaces such as a neck support pillow or a backrest cushion of a seat.

Such designs would guarantee that PV would function with high efficiency at the BZ of the protected person. The PV ATD used in this study can only obtain a clean-air delivery efficiency of 40%, and was shown to not be very effective in protecting an exposed occupant against infectious particles, especially at a low air-flow rate. Higher efficiency PV systems may help to minimize the infection risk for an occupant.

Another way to increase the benefits of PV is to block the transmission route between two occupants. From Figs. 9 and 13, it can be seen that direct exposure occurs when the exhalation flow penetrates the exposed occupant's BZ. If a partition with sufficient height can be set between the occupants to block the penetration of the exhaled flow, the possibility of PV's direct entrainment of the exhaled flow from another occupant will be substantially lowered. Such partitions are commonly used in office rooms, and thus could also be used in other situations.

PV combined with personalized exhaust (PE) may serve as another

means to control transmission of infectious particles. That is, PV used only for the infector may actually facilitate the transport of exhaled infection particles. Although the resulting increased infection possibility was found to be limited, PV's promotion of the mixing of exhaled pathogens with room air should be avoided. In this context, PE used by occupants may directly perturb the dispersion of exhaled pathogens and should be effective in infectious source control [65]. Melikov and Dzhartov [66] developed an air distribution method for capturing exhaled air by using the "push and pull" ventilation principle. Briefly, a front PV nozzle supplied clean air to the occupant and pushed the exhaled air to disperse both sideways and backwards. The PE of two headrest exhaust terminals removed the pushed exhaled air before it mixed with the surrounding air. This design combined the benefits of PV and PE and resulted in a substantial decrease in the concentration of infectious particles in the ambient air. A combination of PV and PE was also found to increase the received amount of clean air from PV [67].

Yang et al. developed two types of PE for positioning on an individual's shoulder or torso, for use in healthcare facilities to reduce doctors' exposure when diagnosing potentially infected patients [68]. If this PE was combined with PV for doctors' (or anyone else's) use, the intake fraction of exhaled contaminant would be less than that achieved with use of PV or PE alone [69]. These findings show that PE [65–69] has excellent performance, and may be another promising solution for airborne transmission control.

4.2. Limitations of this study

The breathing from a manikin could be different to that of humans [30], which means that these findings deviate from the reality in some aspects. In addition, it was assumed that the average concentration of droplets reaching human subjects would all be infectious, but this would not be true in reality because not all of the expelled droplets would contain infectious particles, which would also lead to over-estimates of the infection risk of influenza A. For mouth breathing, most measurements from human subjects have a downward flow-trend angle rather than the upward flow from the manikin. Moreover, the propagation distance of exhaled flow in humans was less than that of the manikin. These deviations would also contribute to overestimation of exposure risk.

The alignments of PV with specific distances and angles in this study are not representative configurations of all PV systems, and thus the conclusions are not generalizable to all PV systems. The performance of PV in disease control could be affected by a number of factors, such as background ventilation, the supplied air temperature and the relative distance between occupants, and these should be investigated in future studies.

5. Conclusions

It was previously reported that PV protection technology was able to mitigate the spread of airborne transmissible disease, but this research area is new. This paper was focused on evaluating the effect of PV on the probability of cross infection between two occupants in close proximity (<1 m). Two scenarios with different alignments of PV were compared. Concerns about the possibility of PV facilitating the transport of exhaled pathogen were examined in two ways.

In the first, the infector was subjected to PV, meaning that the PV flow interacted with the exhaled flow from the source, resulting in accelerated mixing of exhaled droplets with room air and occasionally increased exposure of the susceptible person to particles. Over 90% of the droplets to which the susceptible person was exposed were derived from indirect transmission when only the source manikin used PV.

In the second, the PV interacted with the infector's exhaled flow, which increased the direct exposure level. When the PV flow fell within the area accessible to the exhalation of the infector, the PV jet entrained more droplets, resulting in an increased direct exposure to the susceptible person of more than 50%.

The infection risk of influenza A was evaluated based on the dose-response model. With a continuous exposure time of 2 h, the infection probability varied from 0.28 to 0.85 according to different PV alignments. PV displayed a potential to reduce infection risk only when PV was operated with a high efficiency and successfully supplied clean air to the breathing zone of the protected person. This was achieved when both the source and target were subject to PV at a flow rate of 9 L/s in both scenarios, indicating that a higher clean air volume and no direct entrainment from the infector's exhalation would aid in protection against disease transmission to the exposed occupant.

The complex interaction of airflows in the microenvironment between occupants was found to affect the efficiency of PV and the transmission of droplets. As PV is a ventilation mode that directly perturbs a human microenvironment, the flow interactions between these airflows should be carefully considered to achieve an optimal design for infection control. Use of PE for infectious source control, measures to block the penetration of exhaled flow and designs for improving the efficiency of PV ATDs would be beneficial to maximize the effective application of PV for airborne disease control within the human microenvironment.

Declaration of competing interest

The authors declare that they have no known competing financial interests or personal relationships that could have appeared to influence the work reported in this paper.

Acknowledgments

This project was financially supported by the National Natural Science Foundation of China (51808555, 51778520), the National Key Research and Development Program of China (2017YFC0702700), the Natural Science Foundation of Shandong Province (ZR2019MEE060), the Opening Fund of State Key Laboratory of Green Building in Western China (LSKF202014) and the Fundamental Research Funds for the Central Universities (18CX02076A, XZY032020029).

Appendix A. Supplementary data

Supplementary data to this article can be found online at https://doi.org/10.1016/j.buildenv.2020.107008.

References

[1] Centers for Disease Control and Prevention, CDC Influenza Programs Protect, 2019. https://www.cdc.gov/flu/pandemic-resources/. accessed 26 November 2019.
[2] R. Tellier, Aerosol transmission of influenza A virus: a review of new studies, J. R. Soc. Interface 6 (2009) S783–S790, https://doi.org/10.1098/rsif.2009.0302.focus.
[3] COVID-19 Epidemic Statistics, 2020. https://voice.baidu.com/act/newpneumonia/newpneumonia/?from=osari_pc_3. accessed 27 April 2020.
[4] C. Xu, X. Luo, C. Yu, S.J. Cao, The 2019-nCoV epidemic control strategies and future challenges of building healthy smart cities, Indoor Built Environ. (2020) 1–6, https://doi.org/10.1177/1420326X20910408. In press.
[5] J. Wei, Y. Li, Airborne spread of infectious agents in the indoor environment, Am. J. Infect. Contr. 44 (2016) S102–S108, https://doi.org/10.1016/j.ajic.2016.06.003.
[6] Y. Li, G.M. Leung, J.W. Tang, X. Yang, C.Y.H. Chao, J.Z. Lin, J.W. Lu, P.V. Nielsen, J. Niu, H. Qian, A.C. Sleigh, H.J. Su, J. Sundell, T.W. Wong, P.L. Yuen, Role of ventilation in airborne transmission of infectious agents in the built environment - a multidisciplinary systematic review, Indoor Air 17 (2007) 2–18, https://doi.org/10.1111/j.1600-0668.2006.00445.x.
[7] J.C. Luongo, K.P. Fennelly, J.A. Keen, Z.J. Zhai, B.W. Jones, S.L. Miller, Role of mechanical ventilation in the airborne transmission of infectious agents in buildings, Indoor Air 26 (2016) 666–678, https://doi.org/10.1111/ina.12267.
[8] Y. Jiang, B. Zhao, X. Li, X. Yang, Z. Zhang, Y. Zhang, Investigating a safe ventilation rate for the prevention of indoor SARS transmission: an attempt based on a simulation approach, Build. Simul. 2 (2009) 281–289.
[9] World Health Organization (WHO), in: J. Atkinson, Y. Chartier, C. Pessoa-Silva, P. Jensen, Y. Li, et al. (Eds.), Natural Ventilation for Infection Control in Health-Care Settings, WHO Publication/Guidelines, WHO Press, Geneva, Switzerland, 2009.

[10] P.V. Nielsen, Control of airborne infectious diseases in ventilated spaces, J. R. Soc. Interface 6 (2009) S747–S755, https://doi.org/10.1098/rsif.2009.0228.focus.

[11] M. Sandberg, A. Kabanshi, H. Wigö, Is building ventilation a process of diluting contaminants or delivering clean air? Indoor Built Environ. (2019) 1–7, https://doi.org/10.1177/1420326X19837340. In press.

[12] A.K. Melikov, Personalized ventilation, Indoor Air 14 (Suppl 7) (2004) 157–167, https://doi.org/10.1111/j.1600-0668.2004.00284.x.

[13] Z.D. Bolashikov, A.K. Melikov, Methods for air cleaning and protection of building occupants from airborne pathogens, Build. Environ. 44 (2009) 1378–1385, https://doi.org/10.1016/j.buildenv.2008.09.001.

[14] ASHRAE Position Document on Airborne Infectious Diseases, 2020. https://www.ashrae.org/file%20library/about/position%20documents/airborne-infectious-diseases.pdf. assessed 20 April 2020.

[15] J. Pantelic, G.N. Sze-To, K.W. Tham, C.Y. Chao, Y.C. Khoo, Personalized ventilation as a control measure for airborne transmissible disease spread, J. R. Soc. Interface 6 (2009) S715–S726, https://doi.org/10.1098/rsif.2009.0311.focus.

[16] R. Cermak, A.K. Melikov, Protection of occupants from exhaled infectious agents and floor material emissions in rooms with personalized and underfloor ventilation, HVAC R Res. 13 (2007) 23–38, https://doi.org/10.1080/10789669.2007.10390942.

[17] C. Habchi, K. Ghali, N. Ghaddar, W. Chakroun, S. Alotaibi, Ceiling personalized ventilation combined with desk fans for reduced direct and indirect cross contamination and efficient use of office space, Energy Convers. Manag. 111 (2016) 158–173, https://doi.org/10.1016/j.enconman.2015.12.067.

[18] P.V. Nielsen, H. Jiang, M. Polak, Bed with integrated personalized ventilation for minimizing cross infection, in: O. Seppänen, J. Säteri (Eds.), Proceedings of Roomvent 2007: Helsinki 13-15 June 2007: Abstract Book. FINVAC Ry, 2007, p. 218.

[19] L. Liu, Y. Li, P.V. Nielsen, R.L. Jensen, J. Wei, Short-range airborne transmission of expiratory droplets between two people, Indoor Air 27 (2016) 452–462, https://doi.org/10.1111/ina.12314.

[20] W. Chen, N. Zhang, J. Wei, H.L. Yen, Y. Li, Short-range airborne route dominates exposure of respiratory infection during close contact, Build. Environ. 176 (2020) 106859, https://doi.org/10.1016/j.buildenv.2020.106859.

[21] X. Li, J. Niu, N. Gao, Co-occupant's exposure to exhaled pollutants with two types of personalized ventilation strategies under mixing and displacement ventilation systems, Indoor Air 23 (2013) 162–171, https://doi.org/10.1111/ina.12005.

[22] D. Licina, A. Melikov, C. Sekhar, T.K. Wai, Human convective boundary layer and its interaction with room ventilation flow, Indoor Air 25 (2004) 21–35, https://doi.org/10.1111/ina.12120.

[23] C. Xu, P.V. Nielsen, L. Liu, R.L. Jensen, G. Gong, Impacts of airflow interactions with thermal boundary layer on performance of personalized ventilation, Build. Environ. 135 (2018) 31–41, https://doi.org/10.1016/j.buildenv.2018.02.048.

[24] C. Xu, L. Liu, Personalized ventilation: one possible solution for airborne infection control in highly occupied space? Indoor Built Environ. 27 (2018) 873–876, https://doi.org/10.1177/1420326X18777383.

[25] B. Yang, A.K. Melikov, A. Kabanshi, C. Zhang, F.S. Bauman, G. Cao, H. Awbi, H. Wigö, J. Niu, K.W.D. Cheong, K.W. Tham, M. Sandberg, P.V. Nielsen, R. Kosonen, R. Yao, S. Kato, S.C. Sekhar, S. Schiavon, T. Karimipanah, X. Li, Z. Lin, A review of advanced air distribution methods-theory, practice, limitations and solutions, Energy Build. 202 (2019) 109359, https://doi.org/10.1016/j.enbuild.2019.109359.

[26] Z.D. Bolashikov, A.K. Melikov, M. Spilak, I. Nastase, A. Meslem, Improved inhaled air quality at reduced ventilation rate by control of airflow interaction at the breathing zone with lobed jets, HVAC R Res. 20 (2014) 238–250, https://doi.org/10.1080/10789669.2013.864919.

[27] Z.D. Bolashikov, A.K. Melikov, W. Kierat, Z. Popiołek, M. Brand, Exposure of health care workers and occupants to coughed airborne pathogens in a double-bed hospital patient room with overhead mixing ventilation, HVAC R Res. 18 (2012) 602–615, https://doi.org/10.1080/10789669.2012.682692.

[28] Z. Bolashikov, A. Melikov, M. Krenek, Control of the free convective flow around the human body for enhanced inhaled air quality: application to a seat-incorporated personalized ventilation unit, HVAC R Res. 16 (2010) 161–188, https://doi.org/10.1080/10789669.2010.10390899.

[29] ISO 14644-1: 2015 (Edition 2) Cleanrooms and Associated Controlled Environments, Publication date, 2015, p. 12.

[30] C. Xu, P.V. Nielsen, G. Gong, L. Liu, R.L. Jensen, Measuring the exhaled breath of a manikin and human subjects, Indoor Air 25 (2015) 188–197, https://doi.org/10.1111/ina.12129.

[31] C. Xu, P.V. Nielsen, G. Gong, R.L. Jensen, L. Liu, Influence of air stability and metabolic rates on exhaled flow, Indoor Air 25 (2015) 198–209, https://doi.org/10.1111/ina.12135.

[32] Z.T. Ai, A.K. Melikov, Airborne spread of expiratory droplet nuclei between the occupants of indoor environments: a review, Indoor Air 28 (2018) 500–524, https://doi.org/10.1111/ina.12465.

[33] J. Pantelic, K.W. Tham, D. Licina, Effectiveness of a personalized ventilation system in reducing personal exposure against directly released simulated cough droplets, Indoor Air 25 (2015) 683-693, https://doi.org/10.1111/ina.12187.

[34] I. Olmedo, P.V. Nielsen, M.R.D. Adana, R.L. Jensen, P. Grzelecki, Distribution of exhaled contaminants and personal exposure in a room using three different air distribution strategies, Indoor Air 22 (2012) 64-76, https://doi.org/10.1111/j.1600-0668.2011.00736.x.

[35] J.M. Villafruela, I. Olmedo, J.F. San José, Influence of human breathing modes on airborne cross infection risk, Build. Environ. 106 (2016) 340–351, https://doi.org/10.1016/j.buildenv.2016.07.005.

[36] R.S. Papineni, F.S. Rosenthal, The size distribution of droplets in the exhaled breath of healthy human subjects, J. Aerosol Med. 10 (1997) 105–116, https://doi.org/10.1089/jam.1997.10.105.

[37] D.A. Edwards, J.C. Man, P. Brand, J.P. Katstra, K. Sommerer, H.A. Stone, E. Nardell, G. Scheuch, Inhaling to mitigate exhaled bioaerosols, Proc. Natl. Acad. Sci. U.S.A. 101 (2004) 17383–17388, https://doi.org/10.1073/pnas.0408159101.

[38] L. Morawska, G.R. Johnson, Z.D. Ristovski, M. Hargreaves, K. Mengersen, S. Corbett, C.Y.H. Chao, Y. Li, D. Katoshevski, Size distribution and sites of origin of droplets expelled from the human respiratory tract during expiratory activities, J. Aerosol Sci. 40 (2009) 256–269, https://doi.org/10.1016/j.jaerosci.2008.11.002.

[39] L. Liu, J. Wei, Y. Li, A. Ooi, Evaporation and dispersion of respiratory droplets from coughing, Indoor Air 27 (2016) 179–190, https://doi.org/10.1111/ina.12297.

[40] M.P. Wan, C.Y.H. Chao, Y.D. Ng, G.N. Sze To, W.C. Yu, Dispersion of expiratory aerosols in a general hospital ward with ceiling mixing type mechanical ventilation system, Aerosol Sci. Technol. 41 (2007) 244–258, https://doi.org/10.1080/02786820601146985.

[41] X. Xie, Y. Li, A.T.Y. Chwang, P.L. Ho, W.H. Seto, How far droplets can move in indoor environments: revisiting the Wells evaporation-falling curve, Indoor Air 17 (2007) 211–225, https://doi.org/10.1111/j.1600-0668.2007.00469.x.

[42] M. Nicas, W. Nazaroff, A. Hubbard, Towards understanding the risk of secondary airborne infection: emission of respirable pathogens, J. Occup. Environ. Hyg. 2 (2005) 143–154, https://doi.org/10.1080/15459620590918466.

[43] M. Duan, L. Liu, G. Da, E. Géhin, P.V. Nielsen, U.M. Weinreich, B. Lin, Y. Wang, T. Zhang, W. Sun, Measuring the administered dose of particles on the facial mucosa of a realistic human model, Indoor Air 30 (2020) 108–116, https://doi.org/10.1111/ina.12612.

[44] S. Asadi, A.S. Wexler, C.D. Cappa, S. Barreda, N.M. Bouvier, W.D. Ristenpart, Aerosol emission and superemission during human speech increase with voice loudness, Sci. Rep-UK 9 (2019) 2348, https://doi.org/10.1038/s41598-019-38808-z.

[45] P.V. Nielsen, Y. Li, M. Buus, F.V. Winther, Risk of cross-infection in a hospital ward with downward ventilation, Build. Environ. 45 (2010) 2008–2014, https://doi.org/10.1016/j.buildenv.2010.02.017.

[46] I. Olmedo, F.A. Berlanga, J.M. Villafruela, M. Ruiz de Adanaa, Experimental variation of the personal exposure in a hospital room influenced by wall heat gains, Build. Environ. 154 (2019) 252–262, https://doi.org/10.1016/j.buildenv.2019.03.008.

[47] P.V. Nielsen, I. Olmedo, M.R.D. Adana, P. Grzelecki, R.L. Jensen, Airborne cross-infection risk between two people standing in surroundings with a vertical temperature gradient, HVAC R Res. 18 (2012) 552–561, https://doi.org/10.1080/10789669.2011.598441.

[48] W.C. Hinds, Aerosol Technology, John Wiley & Sons, Inc., New York, NY, 1999.

[49] G.N. Sze To, M.P. Wan, C.Y.H. Chao, F. Wei, S.C.T. Yu, J.K.C. Kwan, A methodology for estimating airborne virus exposures in indoor environments using the spatial distribution of expiratory aerosols and virus viability characteristics, Indoor Air 18 (2008) 425–438, https://doi.org/10.1111/j.1600-0668.2008.00544.x.

[50] W.C. Day, R.F. Berendt, Experimental tularemia in Macaca mulatta: relationship of aerosol particle size to the infectivity of airborne pasteurella tularensis, Infect. Immun. 5 (1972) 77–82.

[51] B.R. Murphy, E.G. Chalhub, S.R. Nusinoff, J. Kasel, R.M. Chanock, Temperature-sensitive mutants of influenza virus. 3. Further characterization of the ts-1 influenza A recombinant (H3N2) virus in man, J. Infect. Dis. 128 (1973) 479–487, https://doi.org/10.1093/infdis/128.4.479.

[52] M.P. Atkinson, L.M. Wein, Quantifying the routes of transmission for pandemic influenza, Bull. Math. Biol. 70 (2008) 820–867, https://doi.org/10.1007/s11538-007-9281-2.

[53] R. H Alford, J.A. Kasel, P.J. Gerone, V. Knight, Human influenza resulting from aerosol inhalation, Proc. Soc. Exp. Biol. Med. 122 (1966) 800–804, https://doi.org/10.3181/00379727-122-31255.

[54] R.G. Douglas, Influenza in man, in: E.D. Kilbourne (Ed.), The Influenza Viruses and Influenza, Academic Press, New York, 1975, pp. 375–447.

[55] J.H. Hemmes, K.C. Winkler, S.M. Kool, Virus survival as a seasonal factor in influenza and poliomyelitis, Nature 188 (1960) 430–431, https://doi.org/10.1007/bf02538737.

[56] C. Xu, P.V. Nielsen, L. Liu, R.L. Jensen, G. Gong, Human exhalation characterization with the aid of schlieren imaging technique, Build. Environ. 112 (2017) 190–199, https://doi.org/10.1016/j.buildenv.2016.11.032.

[57] F.A. Berlanga, L. Liu, P.V. Nielsen, R.L. Jensen, A. Costa, I. Olmedo, M.R. de Adana, Influence of the geometry of the airways on the characterization of exhalation flows. Comparison between two different airway complexity levels performing two different breathing functions, Sustain. Cities Soc. 53 (2020) 101874, https://doi.org/10.1016/j.scs.2019.101874.

[58] C.N. Haas, J.B. Rose, C.P. Gerba, Quantitative Microbial Risk Assessment, John Wiley & Sons, Inc., New York, NY, 1999.

[59] H.E. Khalifa, M.I. Janos, J.F.D. Iii, Experimental investigation of reduced-mixing personal ventilation jets, Build. Environ. 44 (8) (2009) 1551–1558, https://doi.org/10.1016/j.buildenv.2008.11.006.

[60] J.S. Russo, T.Q. Dang, H.E. Khalifa, Computational analysis of reduced-mixing personal ventilation jets, Build. Environ. 44 (8) (2009) 1559–1567, https://doi.org/10.1016/j.buildenv.2008.11.005.

[61] Z.D. Bolashikov, M. Barova, A.K. Melikov, Wearable personal exhaust ventilation: improved IAQ and reduced exposure to air exhaled from a sick doctor, Sci. Technol. Built. Environ. 21 (2015) 1117-1125, https://doi.org/10.1080/23744731.2015.1091270.

[62] A.K. Melikov, T. Ivanova, G. Stefanova, Seat incorporated personalized ventilation, Proceedings Room Vent (2007) 1318.
[63] J. Niu, N. Gao, P. Ma, H. Zuo, Experimental study on a chair-based personalized ventilation system, Build. Environ. 42 (2) (2007) 913–925, https://doi.org/10.1016/j.buildenv.2005.10.011.
[64] Z.D. Bolashikov, L. Nikolaev, A.K. Melikov, J. Kaczmarczyk, P.O. Fanger, Personalized ventilation: air terminal devices with high efficiency, Proceedings of Healthy Building, Singapore 2 (2003) 850–855.
[65] R.K. Dygert, T.Q. Dang, Mitigation of cross-contamination in an aircraft cabin via localized exhaust, Build. Environ. 45 (2010) 2015–2026, https://doi.org/10.1016/j.buildenv.2010.01.014.
[66] A.K. Melikov, V. Dzhartov, Advanced air distribution for minimizing airborne cross-infection in aircraft cabins, HVAC R Res. 19 (2013) 926–933, https://doi.org/10.1080/10789669.2013.818468.
[67] J. Yang, C. Sekhar, D. Cheong, B. Raphael, Performance evaluation of an integrated Personalized Ventilation-Personalized Exhaust system in conjunction with two background ventilation systems, Build. Environ. 78 (2014) 103–110, https://doi.org/10.1016/j.buildenv.2014.04.015.
[68] J. Yang, C. Sekhar, D.K.W. Cheong, B. Raphael, A time-based analysis of the personalized exhaust system for airborne infection control in healthcare settings, Sci. Technol. Built. Environ. 21 (2015) 172-178, https://doi.org/10.1080/10789669.2014.976511.
[69] J. Yang, S.C. Sekhar, K.W. D Cheong, B. Raphael, Performance evaluation of a novel personalized ventilation-personalized exhaust system for airborne infection control, Indoor Air 25 (2015) 176–187, https://doi.org/10.1111/ina.12127.